

## EXPERIMENTAL INVESTIGATION OF A FORCED CONVECTION HEAT TRANSFER OF THE ORGANIC FLUID R-125 AT SUPERCRITICAL PRESSURES AND UNDER ORGANIC RANKINE CYCLE CONDITIONS

Lazova M.\*, Kaya A., Billiet M., Lecompte S. and De Paepe M.

\*Author for correspondence

Department of Flow, Heat and Combustion Mechanics,

Ghent University - UGent,

Ghent, 9000,

Belgium,

E-mail: marija.lazova@ugent.be

### ABSTRACT

The organic Rankine cycle (ORC) is a suitable technology for utilizing low-grade temperature heat sources of  $\sim 100$  °C from various industry processes. In the ORC cycle an organic fluid with a lower boiling point is used as a working medium. The performance of the ORCs has advanced significantly in the last decades. However, there is still a possibility of improving the efficiency of this cycle. The supercritical heat transfer in the heat exchanger ensures better thermal match between the heating and working fluids temperatures glides in the heat exchanger. Hence, better understanding of the heat transfer phenomena to a fluid at supercritical state in a horizontal flow and in a large diameter tube is of great importance. Therefore, the tests are performed in a counter-current tube-in-tube test section positioned horizontally with a total length of 4 m and a tube diameter of 0.0286 m. R-125 is used as a working fluid in the experiments. During the measurements the temperature of the heating fluid was 90 °C, the mass flow rate and the pressure of the working fluid R-125 was in the range of 0.2–0.3 kg/s and 38–55 bar respectively. Furthermore, results from the pressure and temperature measurements obtained at the inlet and at the outlet of the test section are reported. The results show that the overall heat transfer coefficient is influenced by the mass flow rate of the organic fluid. At pressures close to the critical pressure of R-125 higher values of the overall heat transfer coefficients are determined. Deteriorated heat transfer is not likely to occur at these operating conditions because the critical heat flux is higher than the one obtained from the measurements. A comparison between the experimental Nusselt number with heat transfer (Nusselt) correlations from the literature is done and the measurement points fall within the uncertainty ranges of both heat transfer correlations.

### INTRODUCTION

In the last 40 years the total primary energy use across the world has increased with 99% and is expected to keep this trend in the years to come. For example in 2014 the industry accounts for about 42.5% of the total primary energy use (International 2016). All industry processes involve losses and according to

the statistical investigations up to 50% is accounted as a waste heat

### NOMENCLATURE

$A$	[m <sup>2</sup> ]	Heat transfer area
$c_p$	[J/kgK]	Specific heat capacity
$G$	[kg/m <sup>2</sup> s]	Mass flux
$h$	[kJ/kg]	Enthalpy
$p$	[bar]	Pressure
$k$	[W/mK]	Thermal conductivity
$LMTD$	[-]	log mean temperature difference
$\dot{m}$	[kg/s]	Mass flow rate
$\mu$	[Pa·s]	Viscosity
$ORC$	[-]	Organic Rankine cycle
$R$	[m <sup>2</sup> K/W]	Thermal resistance
$T$	[°C]	Temperature
$U$	[W/m <sup>2</sup> K]	Overall heat transfer coefficient
$q$	[kW/m <sup>2</sup> ]	Heat flux
$\dot{Q}$	[kW]	Heat transfer rate

#### Special characters

$\Delta$	[-]	Difference
----------	-----	------------

#### Dimensionless numbers

$Nu$	Nusselt number
$Re$	Reynolds number
$Pr$	Prandtl number

#### Subscripts

$b$	Bulk
$cr$	Critical
$fo$	Fouling
$hf$	Heating fluid
$i$	Inner
$in$	Inlet conditions
$ov$	Overall
$o$	Outer
$pc$	Pseudo-critical
$w$	Wall
$wf$	Working fluid
$out$	Outlet conditions

(Hung, Shai et al. 1997). If this energy in the form of low-grade waste heat is recovered, it would considerably reduce the energy demand in the industry. The organic Rankine cycle (ORC) is an advanced technology that can utilize low-grade temperature heat sources of  $\sim 100$  °C and converts into electricity. In this cycle, organic fluids are employed with a

lower critical pressure and temperature compared to water that is used in a classical Rankine cycle. Even though ORC is an advanced technology there is still possibility to improve its performance. One way to increase the efficiency of this cycle is possible by ensuring better thermal match in the heat exchanger between the heat source and the working fluids temperature glides. In Figure 1, a T-s diagram and a schematic of a transcritical ORC with the basic components that includes a pump, a heat exchanger, an expander and a condenser. The organic fluid is compressed above its critical pressure (1-2), during the heat addition process in the heat exchanger the fluid is heated up (vaporized) beyond its critical temperature (2-3), then the vapour is expanded (3-4) and at the end condensed (4-1) with which the cycle closes. In this case there is no phase change because the two-phase region is omitted.

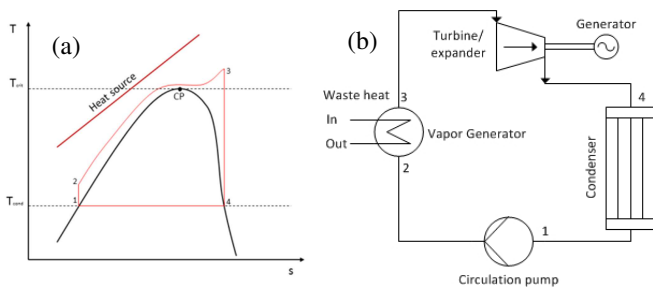


**Figure 1** (a) T-s diagram; (b) Schematic overview of the transcritical ORC

In many theoretical studies, related to low-grade heat source ( $\sim 100$  °C) transcritical ORC cycles, the organic fluid R-125 is considered as a working medium because of the low critical pressure and temperature (36.2 bar and 66 °C). Baik *et al.* (Baik 2011) did a performance comparison of R-125 and CO<sub>2</sub> with a heat source temperature of 100 °C. The pressure drop characteristics and heat transfer rate were considered by using discretized heat exchanger model. The working fluid CO<sub>2</sub> has a better heat transfer and pressure drop characteristics compared to R-125. However, R-125 is favourable fluid because more net electrical power is produced (14%) due to the lower pumping power. This is caused by the lower critical pressure of R-125 ( $p_{cr,R-125}=36.2$  bar) compared to the critical pressure of CO<sub>2</sub> ( $p_{cr,CO_2}=73.9$  bar). In another study (Quoilin 2011) the power output of several organic fluids such as R-125 and a number of HFC fluids was compared and optimized in a simulation model. R-125 was used in a transcritical ORC and the other fluids in a subcritical ORC. The results show that the power output of R-125 is higher compared to the subcritical ORC when the total overall conductance TOC is higher than 35 kW/K. Additionally, Gu *et al.* (Gu and Sato 2002) compared the performance of R-125 with R134a in a low-temperature geothermal power generation in a transcritical ORC. When comparing with R134a then the R-125 has a lower power output. Zhang *et al.* (Zhang 2011) performed a parametric optimization study for geothermal power generation for a number of working fluids.

The working fluid R-125 was suggested as the most cost effective approach for transcritical ORCs. Therefore, in order to determine the supercritical heat transfer characteristics to an organic fluid under ORC conditions the R-125 was selected. This fluid has beneficial thermo-physical properties and low critical pressure and temperature of 36.2 bar and 66 °C.

In the literature there is a lack of experimental data regarding heat transfer and pressure drop measurements to organic fluids (HFC) which are tested under (transcritical) ORC conditions. In the previous work water and CO<sub>2</sub> were used as working fluids and most of the heat transfer correlations are valid for these fluids. Furthermore, the focus in the existing experimental research is on small tube diameters positioned vertically and different applications. However, the aim of this study is to investigate the heat transfer characteristics at supercritical pressures in a test section with large tube diameter of 0.0286 m that is positioned horizontally.

## SUPERCritical HEAT TRANSFER

Research activities about heat transfer to fluids at supercritical pressure started from the early 50's and in the early 70's (Schmidt, Eckert *et al.* 1946). The supercritical fluids undergo significant variations of the thermo-physical properties (density, specific heat capacity, viscosity, thermal conductivity) at near-critical region. These changes of the organic fluid R-125 are depicted in Figure 2. Particularly, the specific heat capacity reaches a peak at the pseudo-critical temperature  $T_{pc}$  and also the density, the viscosity and the thermal conductivity vary considerably within a small temperature range near the  $T_{pc}$ .

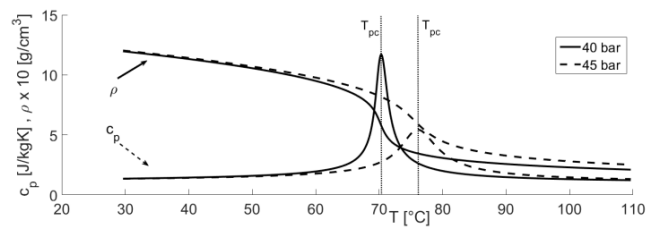


**Figure 2** Thermo-physical property variation of R-125

Moreover, there are several organic fluids that have been tested (R134a, R-404A, R-410A, R-22) under supercritical conditions in either heating or cooling applications. Garimella *et al.* (Garimella 2006) performed experimental investigation regarding supercritical heat transfer to the organic fluids R-404A and R-410A in a horizontal flow and in cooling applications. In his work small diameter tubes in the range between 0.76–3.05 mm were tested and the proposed heat transfer correlation is applicable for pressure  $1.0 < p_{cr} < 1.2$ . An experimental heat transfer investigation of R134a at supercritical pressure between 45–55 bar in cooling application was conducted by Zhao and Jiang (Zhao 2011). The inner diameter of the stainless steel tube is 4.01 mm. The tests had been done at different mass fluxes and a new correlation is proposed based on the measured data. Furthermore, an experimental investigation of the heat transfer characteristics of

R-22 and ethanol in small vertical tubes was conducted in 2012 (Jiang 2012). From the results it was concluded that the frictional pressure drop is more significant for R-22 than for ethanol, while the local heat transfer coefficient increases as the enthalpy increases for both fluids.

There are several general characteristics: the heat flux, the mass flux, the tube diameter, the flow direction and the buoyancy that have an influence on heat transfer to a fluid at supercritical state. Yamagata (Yamagata, Nishikawa et al. 1972) showed that at low heat fluxes, heat transfer is enhanced near the pseudo-critical line. However, heat transfer deterioration happened at high heat fluxes.

## EXPERIMENTAL TEST RIG

A basic layout of the experimental facility iSCORE built at Ghent University is presented in Figure 3. It consists of three different fluid loops: *heating*, *cooling* and *experimental* loop.

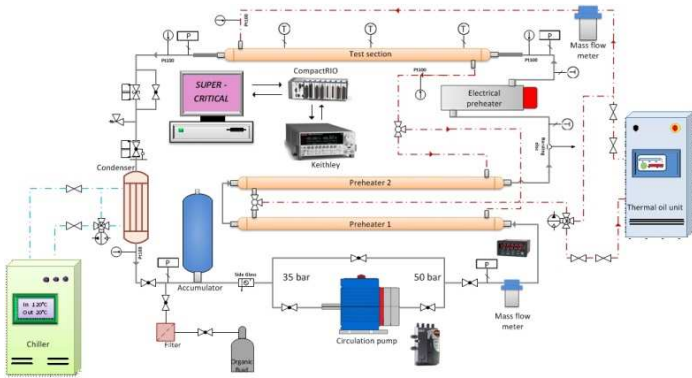


Figure 3 Schematic overview of the test rig “iSCORE”

The heat source is provided by a thermal oil heater with a power of 20 kW. This thermal heater is a compact unit where the low synthetic thermal oil Terminol ADX10 is electrically heated and pumped to the experimental loop which provides a uniform heat transfer in the test section.

A 37 kW chiller is used to regulate the temperature of the cold source which is a mixture of water/glycol that is provided to the condenser to sub-cool the organic fluid (R-125).

In the experimental loop, the test section is positioned horizontally and is equipped with pressure and temperature sensors. A positive displacement (volumetric) pump is used for circulation of the working (organic) fluid which is controlled by a frequency controller. The working fluid is at first pressurized (compressed) above its critical pressure and heated up in the preheaters. In the installation there are two tube-in-tube preheaters and one in-line electrical preheater with a capacity of 10 kW. The tube-in-tube preheaters can be by-passed and utilized if there is a need during the measurements. However, the organic fluid's inlet temperature is controlled by the electrical in-line heater. Two Coriolis mass flow meters are used to measure the mass flow rate of the working and heating fluid respectively. Furthermore, there are many components installed to control the safe operation of the test set-up.

## Test section

The test section is constructed as a horizontal counter-current tube-in-tube heat exchanger where the working fluid flows in the inner tube and the heating fluid (thermal oil) in the annulus which is depicted in Figure 4.

The inner tube is made out of copper alloy tube with the following dimensions: outer diameter of 0.0286 m, thickness of 0.0019 m and heating length of 4 m ( $L/D_i=162$ ). Moreover, for fully-developed flow, the test section is connected with unheated adiabatic test section with a length of 1 m. Measurements in the test section are performed with a large number of sensors. Along the test section, on eleven equal distances of 0.33 m, T-type thermocouples are positioned to measure the bulk temperature of the organic fluid R-125.

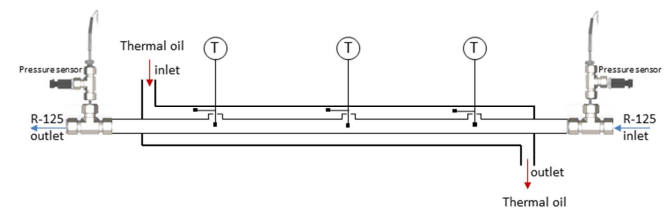


Figure 4 Test section

Furthermore, three thermocouples type K measure the bulk temperature of the thermal oil in the annulus and are placed at a distance of 1 m. To reduce the heat losses to the environment the tubing of the system is insulated with an insulation material with thermal conductivity of 0.04 W/mK.

## DATA REDUCTION METHOD AND ERROR ANALYSIS

### Heat transfer coefficient

The energy balance is determined by employing the Equations (1) and (2), taking into account the counter-current flow:

$$\dot{Q}_{hf} = \dot{m}_{hf} c_p (T_{hf,in} - T_{hf,out}) \quad (1)$$

$$\dot{Q}_{wf} = \dot{m}_{wf} (h_{wf,out} - h_{wf,in}) \quad (2)$$

where  $\dot{Q}$  is the heat transfer rate,  $\dot{m}$  is the mass flow rate of the working and heating fluid respectively. The enthalpy change of the working fluid is  $h$  and the temperature of the heating fluid is  $T_{hf}$ . The overall heat transfer coefficient in the test section is determined by using the log mean temperature difference (*LMTD*) method, Equations (3) and (4):

$$U = \dot{Q}_{wf} / (A \cdot LMTD) \quad (3)$$

$$LMTD = (\Delta T_1 - \Delta T_2) / \ln(\Delta T_1 / \Delta T_2) \quad (4)$$

where  $U$  is the overall heat transfer coefficient,  $\dot{Q}_{wf}$  is the heat transfer rate at the working fluid side,  $A$  is the total heat transfer surface area,  $\Delta T$  is the temperature difference ( $\Delta T_1 = T_{hf,in} - T_{wf,out}$ ) and ( $\Delta T_2 = T_{hf,out} - T_{wf,in}$ ).

The overall heat flux  $q$  from the measurements is determined by the following Equation (5).

$$q = \dot{Q}_{wf} / A \quad (5)$$

Furthermore, in order to determine the Nusselt number of the working fluid from the measurements the following steps were applied. The overall thermal resistance  $R_{ov}$  is expressed with Equation (6). It represents a sum of the thermal resistances corresponding to outer convection  $R_o$ , the tube wall  $R_w$  and the internal convection  $R_i$  resistances, while the internal  $R_{fo,i}$  and outer  $R_{fo,o}$  fouling resistances are neglected (due to the new installation).

$$R_{ov} = R_o + R_w + R_i + R_{fo,i} + R_{fo,o} \quad (6)$$

By employing the proper expressions, Equation (6) can be rewritten as the Equation (7).

$$\frac{1}{UA} = \frac{1}{htc_o A_o} + \frac{\ln(d_o/d_i)}{2\pi\kappa L} + \frac{1}{htc_i A_i} \quad (7)$$

where the left side of the equation expresses the overall heat transfer resistance as a function of the overall heat transfer coefficient  $U$  and the surface area  $A$ . For calculating the overall heat transfer coefficient the outer surface area of the tube is taken into account  $A_o$ . While on the right side of the equation  $htc_o$  and  $htc_i$  are the outer and internal convection heat transfer coefficients,  $d_i$  and  $d_o$  are the inner and outer tube diameters,  $\kappa$  is the wall thermal conductivity of the tube,  $L$  is the length of the tube and  $A_i$  is the inner tube surface area. With this equation the convection heat transfer coefficient at the working fluid side  $htc_i$  is computed.

The bulk working and heating fluid temperatures  $T_{b,wf}$ ,  $T_{b,hf}$  are computed by employing the Equations (8), (9).

$$T_{b,wf} = (T_{wf\_in} + T_{wf\_out}) / 2 \quad (8)$$

$$T_{b,hf} = (T_{hf\_in} + T_{hf\_out}) / 2 \quad (9)$$

In order to determine the wall temperatures  $T_w$ ,  $T_{w,out}$ ,  $T_{w,in}$  at the inner and outer wall side the following equations were applied:

$$q = (T_{hf} - T_{w,out}) / 1 / htc_o \quad (10)$$

$$q = (T_{w,in} - T_{wf}) / (1 / htc_o \cdot d_o / d_i) \quad (11)$$

$$T_w = (T_{w,out} + T_{w,in}) / 2 \quad (12)$$

The convection heat transfer coefficient  $htc_o$  at the heating fluid side can be determined with a heat transfer correlation deduced by Gniellinski (Incropera and DeWitt 1990) which is derived for fully developed turbulent flow and is presented with the Equation (13).

$$Nu = \frac{(f/8)(Re-1000)Pr}{1+127(f/8)^{0.5}(Pr^{2/3}-1)} \quad (13)$$

where  $Re$  is the Reynolds number ( $Re = \frac{\dot{m}_{wf}}{A \cdot \mu}$ ),  $Pr$  is the Prandtl number ( $Pr = \frac{c_p \mu}{k}$ ) and  $f$  is the friction factor ( $f = 1 / (0.79 \cdot \ln(Re) - 1.64)^2$ ). After determining the values of the parameters mentioned in the text above, the experimental Nusselt number at the working fluid side can be calculated with the following Equation (14):

$$Nu = \frac{htc_i \cdot d_{hyd}}{\lambda_{b,wf}} \quad (14)$$

where  $d_{hyd,wf}$  is the hydraulic diameter of the working fluid which in this case is the inner tube diameter  $d_i$  and  $\lambda_{b,wf}$  is the thermal conductivity of the working fluid at bulk temperatures.

### Measurement strategy and Error analysis

Heat transfer and pressure drop measurements over the test section are performed under supercritical conditions with mass flux and heat flux changes with a large number of sensors. However, in this work only the results of the temperature and pressure measurements at the inlet/outlet of the test section are reported. The temperature range of the heat source (thermal oil) was 90 °C while the inlet temperature of the working fluid was between 45–60 °C. The pressure of the heat source was stable at 3 bar while the pressure of the working fluid R-125 varied between 37.5–46 bar. The temperatures at the inlet and the outlet of the test section (heating / working fluid side) are measured by four thermocouples, type Pt100. The minimum and maximum temperature drop of the heating fluid along the test section is 0.8 °C and 3 °C, respectively. The uncertainty of the temperature measurements depends from the accuracy of the Pt100's placed at the test section. All temperature sensors (Pt100) are re-calibrated in-house and their uncertainty is 0.07 °C. The pressure drop over the test section is measured by two pressure transducers (GE UNIK 5000). These pressure sensors have an absolute pressure range between 0–60 bar and are denoted by a P-symbol in the test set-up layout. The uncertainty in the pressure drop is mainly determined by the accuracy of the pressure transducers, which is 0.1% FS BFL (Full Scale Best Fitting Line). Thus the measured pressure drop from experiments is 5.2–9.4 kPa with a relative uncertainty of  $\pm 1.5\%$ . The mass flow rate of the heating and working fluid was measured by two Coriolis mass flow meters and it was in the range of 0.2–2.1 kg/s. All signals are collected by a data acquisition system. Table 1. gives an overview of the corresponding experimental uncertainties.

**Table 1.** Experimental uncertainties.

Parameter	Range	Relative error (%)
Heat input	5–10 kW	2.62
Pressure	37.5–46 bar	1.5
Temperature	45–100 °C	3.71
Mass flow rate	0.2–2.1 kg/s	2.00

The heat (energy) balance between the heating fluid and the working fluid was smaller than 2% away from the critical region. However, the measurements at near-critical and supercritical conditions showed a larger difference in the energy balance (20%) mainly because the enthalpy's uncertainty around the critical region is high.

The uncertainty of the overall heat transfer coefficients is determined by the heat transferred (heat fluxes) and it depends from the working and organic fluids temperatures and mass flow rates. The mean uncertainty on the resulting overall heat transfer coefficient is 11.9%. CoolProp (Bell 2014) was used for the calculation of the thermo-physical properties of the organic fluid R-125. The density and the specific heat capacity have an overall accuracy of 0.05% and 0.5% respectively. This is valid with exclusion of the critical region. The uncertainties in density around the critical region are generally 0.5%, but when compared to experimental data can exceed 5%. The isobaric specific heat capacity has an uncertainty of 1% in the critical region. Uncertainties of the Nusselt number of 9% up to 25% are found from the measurements at supercritical conditions with an average deviation of 12.7%.

## RESULTS AND DISCUSSION

### Influence of the mass flow rate to the heat transfer rate at different pressure

The variations of the heat transfer rate with the mass flow rate changes at different pressures over the test section are depicted in Figure 5.

For all set of measurements the heating fluid temperature was stable at 90 °C ensuring supercritical heat transfer to the working fluid R-125. The pressure at the inlet of the test section was in the range of 37.5–46 bar, mass flow rate 0.19 – 0.30 kg/s. From the results, it is evident that the mass flow rate has a significant influence on the overall heat transfer coefficient. At higher mass flow rate of the working fluid R-125, the overall heat transfer coefficient increases as well. However, it is apparent from Figure 5 that the overall heat transfer coefficient at a mass flow rate of 0.3 kg/s and inlet pressure of 43 bar has the highest value. Close to the critical pressure of R-125 (37.5 bar) and a mass flow rate of 0.25 kg/s there is also a peak in the value of the overall heat transfer coefficient. The reason for reaching higher value of the overall heat transfer coefficient at these conditions is the fact that these results are obtained at supercritical pressure and close to the pseudo-critical temperature  $T_{pc}$  of the working fluid. At pseudo-critical temperature  $T_{pc}$  the specific heat capacity has its maximum value.

By obtaining local temperature measurements and determining the local heat transfer coefficients it will be possible to determine the location where the pick of the specific heat capacity occurs and approaches the pseudo-critical temperature which enhances the local heat transfer coefficient and hence the heat transfer rate

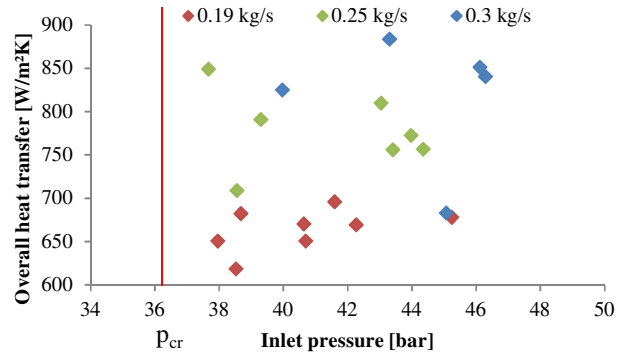


Figure 5 Overall heat transfer coefficients vs. mass flow rates

### Determining the effects of wall temperature

The thermo-physical properties of the working (organic) fluid at supercritical pressures strongly depend on the fluid's and wall's temperature changes. Heat transfer deterioration occurs when the bulk temperature of the working fluid is below the pseudo-critical temperature and the wall temperature significantly exceeds the pseudo-critical temperature. According to the results from the measurements, the wall temperature is higher than the bulk fluid temperature of the working fluid. The difference is between 12–18 °C ( $T_{wf,b} \sim 55$  °C;  $T_{wall} \sim 75$  °C). Therefore, determining if there is occurrence of the effects such as heat transfer deterioration which appears in large increase of the tube wall temperature is of great importance.

An estimation of the “pseudo-critical” wall heat flux is presented with the Equation (15) which is proposed by Styrikovich *et al.* (M.A. Styrikovich 1967).

$$q_{critical} = 580 \cdot G \text{ [W/m}^2\text{]} \quad (15)$$

where  $q$  is the “critical heat flux” and  $G$  is the mass flux of the working fluid.

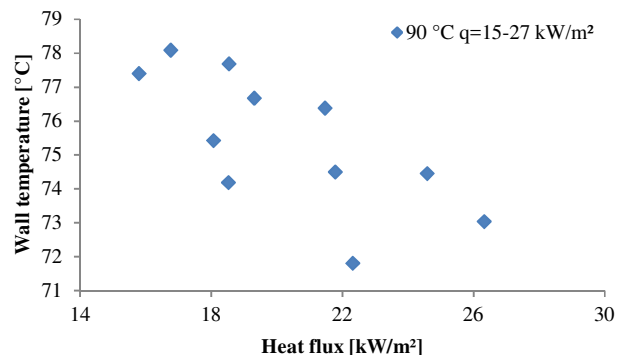


Figure 6 Evaluation the effects of the wall temperature at different heat fluxes

The deteriorated heat transfer regime appears at critical (high) heat flux which in this case would be 372 kW/m<sup>2</sup>. From the measurements it can be concluded that the heat flux obtained from the measurements with a heat source temperature

of 90 °C is significantly lower than the critical heat flux determined by Equation (13) and the experimental heat flux is in the range of 15–27 kW/m<sup>2</sup>. This shows that a deteriorated heat transfer is not likely to occur in these operating conditions. However, from the local heat transfer measurements this phenomenon could be analyzed in detail.

### Comparison of the experimental Nusselt number with heat transfer correlations from literature

The results obtained from the measurements are compared with two heat transfer correlations of Dittus-Boelter type from literature. These two heat transfer (Nusselt) correlations developed by Jackson and Fewster (Jackson 1979,) and Shitsman (Shitsman 1974) were derived for horizontal flow by employing water and CO<sub>2</sub> as working fluids. Both heat transfer correlations were used for sizing the test set-up “iSCORE”. The selected heat transfer correlations are presented in Table 2.

**Table 2** Heat transfer correlations used for the comparison with the experimental Nu number

Author Reference	Correlation	Error
Jackson and Fewster (Jackson 1979,)	$Nu_b = 0.0183Re_b^{0.82}\overline{Pr}^{0.5}\left(\frac{\rho_w}{\rho_b}\right)^{0.3}$	±20%
Shitsman (Shitsman 1974)	$Nu_b = 0.023Re_b^{0.8}Pr_{min}^{0.8}$	±25%

The comparison of the experimental Nusselt number with the (Nusselt) heat transfer correlations is presented in Figure 7.

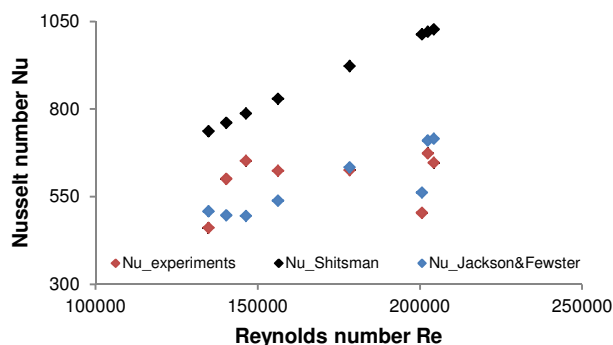


**Figure 7** Comparison of the experimental Nu number with the (Nu) heat transfer correlation from literature

The deviation of these heat transfer correlations is in the range of ±20–25 %. However, the uncertainties of the experimental Nusselt number obtained at supercritical conditions are in the range of 9% up to 25% with an average deviation of 12.7%. From Figure 7 it can be concluded that most of the measurement points fall within the results from both heat transfer correlations from the literature. However, in order to make more precise comparison, determining local heat

transfer coefficients and hence deriving a heat transfer correlation is essential and is part of the future work.

### CONCLUSION

In this article, preliminary results from the forced convection heat transfer measurements at supercritical state, done on the new test set-up are reported. Utilization of low-temperature heating fluid of 90 °C and ensuring supercritical heat transfer in the test section was achieved. At higher mass flow rates the overall heat transfer coefficient reaches highest values. However, at supercritical pressure and bulk fluid temperatures close to the pseudo-critical temperature there is a pick of the heat transfer coefficient. Determining the wall effects on the heat transfer mechanisms is also reported where the conclusion is that occurrence of “pseudo-critical” heat flux and hence deteriorated heat transfer is not likely to occur at these operating conditions. Furthermore, a comparison of the Nusselt number obtained from the experiments with two heat transfer correlations from literature is conducted. The results show that the measurement points fall within the results from both heat transfer correlations. A next step of this research is obtaining local heat transfer measurements and deriving a new correlation for designing supercritical heat exchangers suitable to operate under (transcritical) organic Rankine cycle (ORC) conditions.

### ACKNOWLEDGEMENTS

The results presented in this paper have been obtained within the frame of the IWT SBO-110006 project The Next Generation Organic Rankine Cycles ([www.orcnext.be](http://www.orcnext.be)), funded by the Institute for the Promotion and Innovation by Science and Technology in Flanders. This financial support is gratefully acknowledged.

### REFERENCES

- Baik, Y.-J. K., Minsung; Chang, Chang Ki; Kim, Sung Jin; (2011). Power-based performance comparison between carbon dioxide and R-125 transcritical cycles for a low-grade heat source *Applied Energy* **88** 892–898. .
- Bell, H. I. W., Jorrit.; Quoilin, Sylvain.; Lemort, Vincent.; (2014). "Pure and Pseudo-pure Fluid Thermophysical Property Evaluation and the Open-Source Thermophysical Property Library CoolProp." *Ind. Eng. Chem. Res.* **53** (6): 2498–2508.
- Garimella, S. (2006). High condensing temperature heat transfer performance of low critical temperature refrigerants. Arlington, Virginia, USA, Air-conditioning and refrigeration technology institute, ARTI 21CR program contract number 610-20060, .
- Gu, Z. and H. Sato (2002). Performance of supercritical cycles for geothermal binary design *Energy Conversion and Management* **43** 961–971.
- Hung, T. C., T. Y. Shai, et al. (1997). "A review of organic rankine cycles (ORCs) for the recovery of low-grade waste heat " *Energy* **22**(7): 661-667.
- Incropera, F. D. and D. P. DeWitt (1990). *Fundamentals of Heat and Mass Transfer*, John Wiley and Sons, New York.
- International, E. A. (2016). "Key world energy statistics." from <https://www.iea.org/publications/freepublications/publication/KeyWorld2016.pdf>.

8. Jackson, J. D., Hall, W.B. (1979). "Forced convection heat transfer to fluids at supercritical pressure." Turbulent Forced Convection in Channels and Rod Bundles 2(published by Hemisphere Publishing Corporation): 563-611.
9. Jiang, P.-X. Z., Chen-Ru. Liu, Bo (2012). "Flow and heat transfer characteristics of R-22 and ethanol at supercritical pressures." The Journal of Supercritical Fluids(70): 75-89.
10. M.A. Styrikovich, T. K. M., Z.L. Miropolskiy (1967). "Problem in the development of designs of supercritical boilers." Teploenergetika 1 **14**(6).
11. Quoilin, S. (2011). Sustainable Energy Conversion Through the Use of Organic Rankine Cycles for Waste Heat Recovery and Solar Applications PhD.
12. Schmidt, E., E. Eckert, et al. (1946). "Heat transfer by liquids near the critical state, AFF Translation." Air Materials Command, Wright Field, Dayton, OH, USA No. 527.
13. Shitsman, M. W. (1974). "Heat transfer to supercritical helium, carbon-dioxide and water. Analysis of thermodynamic and transport properties and experimental data." Cryogenics **14**(2): 77-83.
14. Yamagata, K., K. Nishikawa, et al. (1972). "Forced convection heat transfer to supercritical water flowing in tubes " International Journal of Heat and Mass Transfer, **15**: pp.2575-2593.
15. Zhang, S. W., H. Guo, T. (2011). "Performance comparison and parametric optimization of subcritical Organic Rankine Cycle (ORC) and transcritical power cycle system for low-temperature geothermal power generation " Applied Energy **88** 2740-2754.
16. Zhao, C. R. J., Pei. Xue.; (2011). "Experimental study of in-tube cooling heat transfer and pressure drop characteristics of R134a at supercritical pressures." Experimental Thermal and Fluid Science **35** (7): 1293 - 1303.